Journal of Catalysis **191,** 401–408 (2000)
doi:10.1006/jcat.1999.2812, available online at http://www.idealibrary.com on IDEAL®

Propane Hydrogenolysis on Sulfur- and Copper-Modified Nickel Catalysts

I. Alstrup, U. E. Petersen, and J. R. Rostrup-Nielsen*,[1]

Haldor Topsøe Research Laboratories, Nymøllevej 55, DK-2800 Lyngby, Denmark

Received September 16, 1999; revised December 20, 1999; accepted December 20, 1999

The rates and selectivity of propane hydrogenolysis on Ni/$MgAl_2O_4$ catalysts modified by preadsorbed sulfur and on Ni/SiO_2 catalysts modified by copper alloying have been measured. On both types of catalysts, the rate of ethane production goes through a maximum at high temperatures. For the NiCu/SiO_2 catalysts, this behavior correlates with the onset of secondary hydrogenolysis of ethane, but not for the sulfur-modified Ni/$MgAl_2O_4$ catalysts. The selectivity for ethane formation on Ni/$MgAl_2O_4$ catalysts was higher with sulfur than without, but a decreasing function of sulfur at high coverage. The selectivity on NiCu/SiO_2 catalysts was found to increase monotonically with the copper content. Comparisons with a previous propane hydrogenolysis study on nickel–copper catalysts with very different surface properties reveal surprising agreements. Our NiCu/SiO_2 catalysts have been shown to be strongly enriched in copper in the surface of the alloy particles after reduction. This is similar to previous results for unsupported NiCu catalysts but in contrast to the NiCu/SiO_2 catalysts used by Dalmon and Martin (*J. Catal.* 66, 31 (1980)), reported to have bulk composition also in the surface after reduction. The hydrogenolysis results of the two NiCu/SiO_2 catalyst studies are, nevertheless, in close agreement, but deviate strongly from the hydrogenolysis results for the unsupported NiCu particles. It is difficult to reconcile the various hydrogenolysis results with simple ensemble models. It is suggested that special sites may dominate hydrogenolysis activity on nickel catalysts. © 2000 Academic Press

Key Words: **hydrogenolysis; propane; C_3H_8; nickel catalysts; Ni/$MgAl_2O_4$; sulfur; NiCu/SiO_2; nickel–copper alloys; ensemble; special sites.**

1. INTRODUCTION

Catalytic hydrogenolysis of hydrocarbons has been studied for more than 60 years. These reactions have in common that a carbon–carbon bond is ruptured via interaction with hydrogen. They have attracted attention partly because such reactions are important in gasoline production, but also because of the fundamental questions they pose. The early studies were primarily focused on the kinetics of the reaction. Later studies focused more on the sensitive dependence of the activity and selectivity on the detailed structure and composition of the catalytic surface. Thus, Carter *et al.* (1) showed that the ethane hydrogenolysis activity of supported nickel catalysts is strongly dependent on the nickel particle size. The variation of the activity of ethane hydrogenolysis from one metal to another was discussed in a review article by Sinfelt (2). In a classical paper, Sinfelt *et al.* (3) showed that the rate of ethane hydrogenolysis on unsupported NiCu alloy catalysts depends strongly on the copper concentration in contrast to the dehydrogenation of benzene, the specific rate of which was shown to be almost independent of the composition of the alloy catalyst. These and many subsequent results led to the suggestions that it is meaningful to distinguish between structure-sensitive and nonsensitive reactions on the basis of the particle size dependence (4) and to distinguish between type I and type II reactions on NiCu alloy catalysts on the basis of whether the reactivity is weakly or strongly dependent on the composition of the alloy catalysts, respectively (5).

The interest of the present authors was to use the hydrogenolysis reaction as a test reaction for the study of ensemble effects (6, 7).

Propane is the simplest alkane that makes possible simultaneous studies of hydrogenolysis activity and selectivity as functions of various changes in the catalyst. Therefore, catalytic hydrogenolysis of propane is particularly suited for the characterization of many catalysts. The kinetics of ethane and propane hydrogenolysis on nickel catalysts has been interpreted using ensemble models. Martin (8) showed that the kinetics of ethane hydrogenolysis on a silica-supported nickel catalyst could be explained by assuming that the rate-limiting step is the dissociative chemisorption of ethane and that this requires a surface ensemble of at least 12 adjacent nickel atoms, not covered by hydrogen. Also, the kinetics of propane hydrogenolysis on the same nickel catalyst could be explained by a similar ensemble model (9). It has been suggested that the average size of ensembles of active nickel atoms on the surface of nickel catalysts may be controlled by adsorption of atoms blocking nickel sites or alloying

[1] To whom correspondence should be addressed. Fax: +45 45 27 29 99. E-mail: jrn@topsoe.dk.

0021-9517/00 $35.00
Copyright © 2000 by Academic Press
All rights of reproduction in any form reserved.

with inactive atoms. Rostrup-Nielsen (10) showed that the rate of carbon formation on a nickel catalyst depends more strongly on the coverage of preadsorbed sulfur than the rate of methane steam re-forming. This was explained by different ensemble requirements of the two reactions. Many studies of catalytic reactions on nickel–copper catalysts have been interpreted in terms of ensemble models. Dalmon and Martin (11) studied ethane, propane, and *n*-butane hydrogenolysis on silica-supported nickel–copper catalysts and found that the dependence on the copper bulk concentration, x, could be described by a factor $(1-x)^N$. N was interpreted as the number of active nickel surface atoms in the ensemble needed for the reaction. These authors concluded that the results could be accounted for by changes of the average size of ensembles of surface nickel atoms due to the dilution by surface copper atoms. It was found that the direct conversion of ethane, propane, and *n*-butane to methane corresponds to $N = 12$, 18, and 20, respectively.

It is usually supposed (8, 9) that the following two hydrogenolysis reactions take place simultaneously:

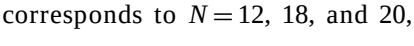

$$C_3H_8 + H_2 \rightarrow CH_4 + C_2H_6 \quad [1]$$

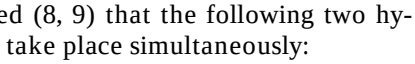

$$C_3H_8 + 2H_2 \rightarrow 3CH_4. \quad [2]$$

If the rate of secondary hydrogenolysis of the ethane formed in reaction [1] is small compared to the rates of reactions [1] and [2], then r_1 and r_2 are almost equal to the rates of reactions [1] and [2], respectively. In the study of Guilleux *et al.* (9), this assumption was supported by the fact that the observed rates were monotonic functions of temperature and that they could be accounted for by simple kinetic expressions. The applicability of this reaction scheme to our results is discussed in the Discussion section. The temperature dependence of the rate constant could be described by an Arrhenius factor, $\exp(-E_0/RT)$, and the hydrogen dependence by a factor of the form $(1-\theta_H)^n$, where θ_H is the hydrogen coverage and n is an integer supposed to represent the number of surface nickel atoms not influenced by adsorbed hydrogen and forming an ensemble needed for propane hydrogenolysis. The pair of parameters (E_0, n) were found to have the values (60 kJ/mol, 17) and (38 kJ/mol, 24) for r_1 and r_2, respectively (9). At a hydrogen pressure of 80 kPa, a propane pressure of 0.27 kPa, and a temperature of 530 K, the apparent activation energy was found to be 176 ± 13 and 213 ± 13 kJ/mol for r_1 and r_2, respectively (9).

In this paper, a study of propane hydrogenolysis on supported nickel catalysts modified either by sulfur chemisorption or by copper alloying is presented and discussed. The results obtained on the nickel–copper alloy catalysts allow us to comment on some studies of hydrogenolysis on nickel–copper alloy catalysts. The notion of active surface ensembles needed for the hydrogenolysis reaction is also debated.

2. EXPERIMENTAL

The influence of sulfur was studied on a commercial nickel catalyst with 13 wt% nickel supported on a magnesium aluminum spinel carrier ($Ni/MgAl_2O_4$) (10). The catalyst was presintered at 1073 K for 96 h in a steam–hydrogen mixture ($H_2O/H_2 = 3$). The sulfur capacity of the reduced catalyst was found to be 160 ppm after sulfidation at 773 K in hydrogen with 10 ppm H_2S. This value corresponds to a nickel area of 0.36 m^2/g catalyst (12), a nickel particle mean diameter of 240 nm, and a dispersion of 0.42%. Sulfur was chemisorbed by exposing the catalyst to a flow of hydrogen with H_2S in the range 0.1–1 ppm at 1073 K. The relevant H_2S/H_2 ratios were selected using the experimental adsorption isotherms (13) and the required sulfidation time was estimated from the Gorring–De Rosset equation (14) and checked by H_2S analysis of the exit gas. The sulfur coverage was determined by sulfur analysis of the respective samples.

$NiCu/SiO_2$ alloy catalysts were prepared by "dry" impregnation as described in Ref. (15). Nickel and copper nitrates were dissolved in water and mixed with silica (Cab-O-Sil H5) to incipient wetness. The mixture was dried at room temperature, calcined at 773 K for 3 h, and finally reduced in H_2 at 773 K for 16 h. The metal content of the catalysts was 20 wt%. The total metal surface area of the reduced catalysts was determined from the sulfur capacity measurements to be 4.6 m^2/g of catalyst, independent of the copper content (15). The metal particle mean diameter was determined from X-ray powder diffraction line broadening to be 18 ± 2 nm for the reduced catalysts, independent of copper content (15). From the metal surface area, a dispersion of 3.9% can be calculated. Table 1 shows the normalized hydrogen chemisorption results for the total amount of hydrogen uptake and for strongly adsorbed hydrogen obtained at room temperature and hydrogen pressures in the range 0.2–30 kPa.

The hydrogenolysis reactions were studied in a quartz microreactor with a 9-mm inner diameter. Three grams of catalyst was used in the $Ni/MgAl_2O_3$ and 0.1 g in the $NiCu/SiO_2$ experiments. Pellets of the catalysts were crushed and particle sizes in the range 0.3–0.5 mm were used in the experiments. A high-purity gas mixture of 1% propane in hydrogen was used as feed after oxygen and water vapor removal by means of a Supelco unit and further

TABLE 1

Hydrogen Uptake on $NiCu/SiO_2$ Catalysts at Room Temperature

Cu at%	Total H_2 uptake, relative	Strongly adsorbed H_2, relative
0	1.0	1.0
0.1	0.98	1.0
1	0.90	0.85
10	0.32	0.18
25	0.23	0.08

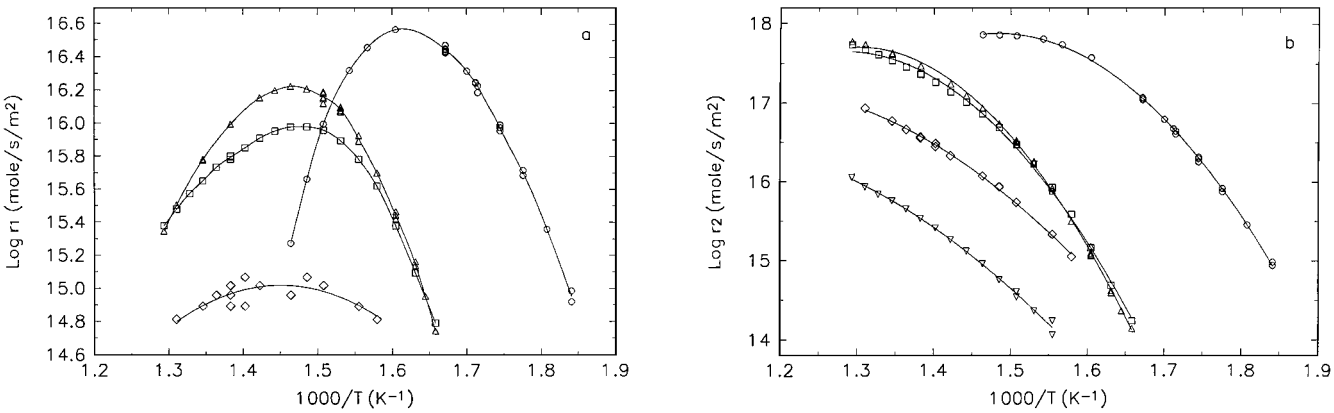

FIG. 1. Arrhenius plot of propane hydrogenolysis rates on $Ni/MgAl_2O_4$ catalysts. Sulfur coverages: 0.0 (○), 0.68 (△), 0.72 (□), 0.88 (◇), 0.94 (▽). (a) r_1 (rate of conversion of C_3H_8 into C_2H_6) and (b) r_2 (total rate of C_3H_8 conversion $- r_1$). The lines are guides for the eyes.

purification by a carbon filter. The reactor was operated at atmospheric pressure. Before the experiments, the catalysts were reduced by heating to 773 K for 1 h in a flow of hydrogen. A gas flow of 10 Nl/h was used in all the experiments.

3. RESULTS

3.1. *$Ni/MgAl_2O_4$ Modified by Sulfur Adsorption*

Figure 1 shows Arrhenius plots of the measured rate of formation of ethane, r_1, by propane hydrogenolysis on $Ni/MgAl_2O_4$ catalysts and r_2, the total rate minus r_1, without sulfur and with sulfur coverages in the range 68–94% of saturation.

The present study covers a larger temperature range (543–773 K) than that reported by Guilleux *et al.* (9), and it is seen that r_1 passes through a maximum for increasing temperature, whereas r_2 increases with temperature in the entire temperature interval considered.

Figure 2 shows the selectivity, $r_1/(r_1+r_2)$, as a function of sulfur coverage for various temperatures in the range 633–683 K. It is seen that the selectivity is, at the lower temperatures, much higher at $\theta_S = 0.68$ than at $\theta_S = 0$, but decreases strongly in the sulfur coverage range 0.68–0.88. The sulfur enhancement of the selectivity increases with temperature. When the sulfur coverage is increased from 0 to 0.68, the selectivity increases by a factor of 10 and 63 at 633 and 683 K, respectively. The lines in Fig. 2 are primarily guides for the eye, but may also be considered as tentative suggestions for sulfur dependencies of the selectivity. However, additional results at lower sulfur coverages are needed in order to establish these dependencies.

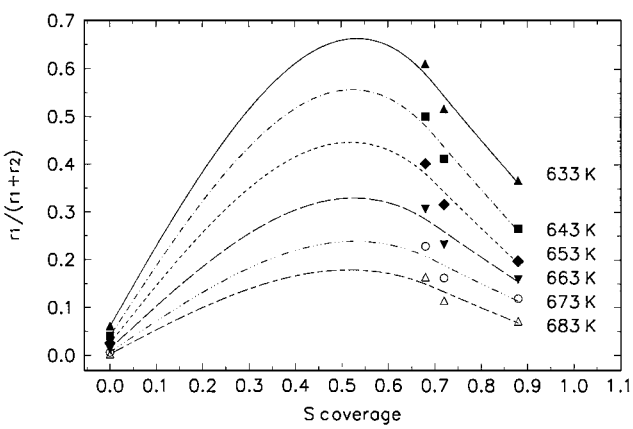

FIG. 2. Selectivity of propane hydrogenolysis on $Ni/MgAl_2O_4$ catalysts as a function of sulfur coverage. Temperature: 633 K (▲), 643 K (■), 653 K (◆), 663 K (▼), 673 K (○), 683 K (△). The lines are guides for the eye.

3.2. *$NiCu/SiO_2$*

Figure 3 shows Arrhenius plots of the rates r_1 and r_2 measured on the series of $NiCu/SiO_2$ catalysts. Again, r_1 passes through a maximum while r_2 increases monotonically with temperature. Figure 4 shows the selectivity as a function of the bulk copper concentration, x, for a number of temperatures in the range 553–603 K. The selectivity increases with increasing copper content and more so at the higher temperatures. When x is increased from 0 to 25%, the selectivity is increased by a factor of 1.6 and 5.3 at 553 and 603 K, respectively. The lines in Fig. 4 are guides for the eye.

4. DISCUSSION

4.1. *Support Effects*

Before discussing the impact of sulfur and copper on the hydrogenolysis of propane on nickel catalysts, we note that the results reveal a big difference between the influence of the two types of support, magnesium–aluminum–spinel and silica. The turnover number of propane hydrogenolysis at 540 K on the silica-supported nickel catalyst is about 50 times larger than that on the magnesium–aluminum–spinel-supported one. This is qualitatively in good agreement with results reported by Burke and Ko (16) and

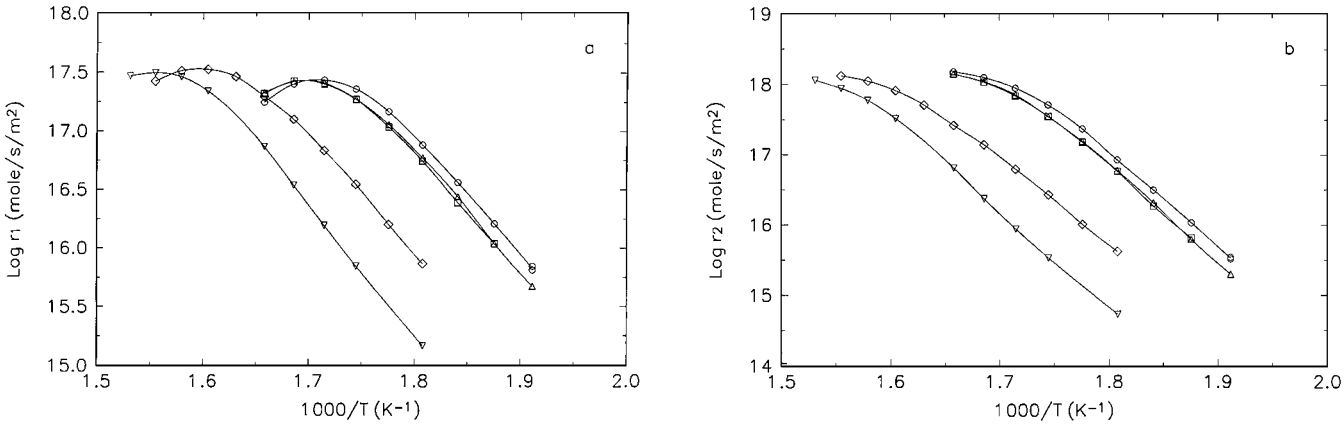

FIG. 3. Arrhenius plot of propane hydrogenolysis rates on $NiCu/SiO_2$ catalysts. Cu/(Ni + Cu) bulk ratio x: 0.0 (○), 0.001 (△), 0.01 (□), 0.1 (◇), 0.25 (▽). (a) r_1 (rate of conversion of C_3H_8 into C_2H_6). (b) r_2 (total rate of C_3H_8 conversion $- r_1$). The lines are guides for the eye.

Jackson *et al.* (17). Burke and Ko (16) studied propane hydrogenolysis on Ni catalysts supported on SiO_2, Nb_2O_5, Nb_2O_5–SiO_2, and TiO_2. Two Ni/SiO_2 catalysts with the same average particle size, but prepared in different ways and reduced at different temperatures, showed activities differing by a factor of 4. This was ascribed to structural differences between the Ni particles of the two catalysts. The authors concluded that the catalyst reduced at the higher temperature had a higher proportion of smooth Ni(111) surface planes, while the Ni particles of the other catalyst had a higher proportion of surface defects. This conclusion was based on an interpretation of infrared spectra obtained in a previous study by Blackmond and Ko (18) of CO and $CO + H_2$ adsorption on the same catalysts. The Ni catalysts supported on Nb_2O_5 or TiO_2 showed activities orders of magnitude lower than those of the SiO_2-supported catalysts. This was ascribed to SMSI (strong metal–support interaction) effects, which are generally believed to be due to decoration of the metal particles by migrating oxide. Jackson *et al.* (17) studied hydrogenolysis of ethane, propane, *n*-butane, and isobutane on Ni/SiO_2, Ni/Al_2O_3, and N/MoO_3 catalysts. They found that the Ni/SiO_2 catalyst was by far the most active and the Ni/MoO_3 catalyst the least active. The dispersion of the Ni/MoO_3 catalyst was similar to that of the Ni/SiO_2 catalyst. These authors suggested tht the very low activity of the Ni/MoO_3 catalyst was due to a support effect or to deposition of carbonaceous species on the Ni particles.

4.2. Reaction Expressions

As mentioned above, it is usually assumed that the reaction expressions [1] and [2] give an adequate description of propane hydrogenolysis on Ni catalysts. The secondary hydrogenolysis of the ethane formed in reaction [1],

$$C_2H_6 + H_2 \rightarrow 2CH_4, \qquad [3]$$

is usually assumed to be negligible. Guilleux *et al.* (9) reported that the ethane turnover number is an order of magnitude smaller than that of propane at 507 K (hydrogen pressure 21.3 kPa and hydrocarbon pressure 3.3 kPa). It is tempting to assume that this does not hold at higher temperatures and that the secondary hydrogenolysis [3] is responsible for the maxima in Figs. 1a and 3a. We shall now check whether our results at the lower temperatures are compatible with the reaction scheme consisting of reactions [1] and [2] and whether the secondary reaction [3] plays a role at the higher temperatures. The rates r_1 and r_2 are calculated from the flow, F, and the concentrations of ethane, C_2, and methane, C_1, by the expressions

$$r_1 = FC_2 \qquad [4]$$

$$r_2 = F(C_1 - C_2)/3. \qquad [5]$$

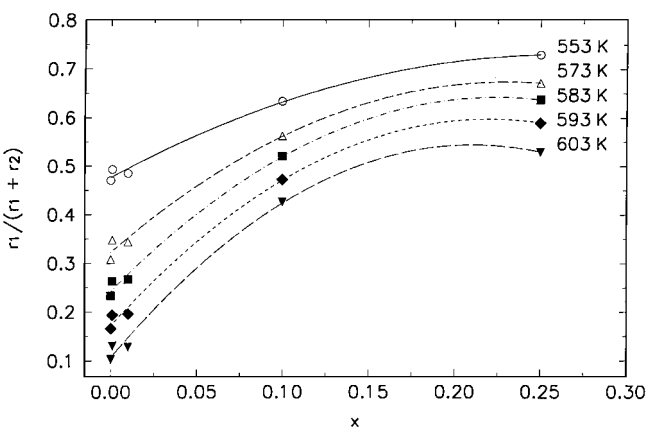

FIG. 4. Selectivity of propane hydrogenolysis on $NiCu/SiO_2$ catalysts as a function of the Cu/(Ni + Cu) bulk ratio x. Temperature: 553 K (○), 573 K (△), 583 K (■), 593 K (◆), 603 K (▼). The lines are guides for the eye.

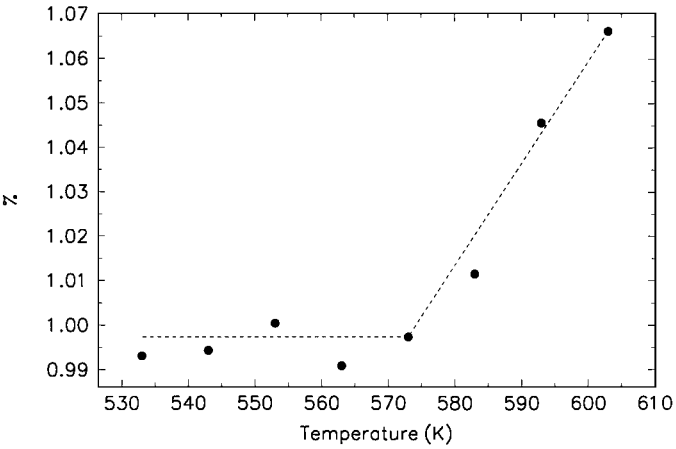

FIG. 5. C_3H_8 hydrogenolysis on $NiCu/SiO_2$ catalyst with 1% Cu. Theoretical percentage of C_3H_8 in feed, calculated from the percentages of C_2H_6 and CH_4 in exit gas assuming only reactions [1] and [2].

If the scheme consisting of reactions [1] and [2] applies and the rate of [3] is negligible, then the sum of C_3H_8 converted into C_2H_6 and CH_4 and the unconverted C_3H_8 is equal to C_3H_8 in the feed, $C_{3,\text{feed}}$,

$$C_{3,\text{feed}} = C_3 + (2C_2 + C_1)/3, \qquad [6]$$

where C_3 is the concentration of C_3H_8 in the exit gas.

We have plotted the right-hand side (rhs) of [6] as function of temperature for all our experiments. The plots of the results for the $Ni/MgAl_2O_4$ catalysts show no clear deviation from a constant, but a considerable scatter of the results ($\pm 10\%$) due to the small rates. We cannot exclude that this scatter may mask a weak increase at higher temperatures. However, all the plots of the results for the $NiCu/SiO_2$ catalysts give clear answers (see the example in Fig. 5): up to a certain temperature, close to the one where r_1 deviates from a straight line in the Arrhenius plots in Fig. 3a, the rhs of [6] is constant and equal to $C_{3,\text{feed}}$, and beyond this temperature the rhs increases linearly. Thus we may conclude that the influence of the secondary hydrogenolysis of ethane may be negligible in the case of $Ni/MgAl_2O_4$ but strong in the case of the silica-supported catalysts and may here be the main cause for the formation of the maxima. In the former case we need another explanation for the formation of the maxima. It may be suggested that reaction [1] consists of at least three steps, an adsorption step, breaking of a C–C bond, and desorption of products, and that the adsorption of C_3H_8 is strongly temperature dependent.

4.3. *$Ni/MgAl_2O_4$ Modified by Sulfur Adsorption*

With increasing sulfur coverage, θ_S, the r_1 maximum moves from 615 K at $\theta_S = 0$ to 690 K at $\theta_S = 0.88$. At the highest sulfur coverage, 0.94, the only product is methane in the temperature range tested (623–773 K). The apparent activation energies, determined at low temperatures, were found to be in the range 210–230 and 250–310 kJ/mol for r_1 and r_2, respectively, without any systematic dependence on the sulfur coverage in the range 0–0.7. The sulfur dependence of r_1 and r_2 is well described by factors of the form $(1-\theta_S)^n$, with n values in the range 2–3 for both reactions in the temperature range 610–680 K. These dependencies are very similar to the sulfur dependence of the rate of steam re-forming on the same type of catalyst, but much weaker than the sulfur dependence of the rate of carbon formation from methane (10). The strongly diminished variation of the selectivity at the higher temperatures reflects the fact that r_2 increases faster with temperature than r_1.

4.4. *$NiCu/SiO_2$*

Figures 3 and 4 show that the influence of copper addition on the rates and selectivity of hydrogenolysis is similar to the influence of sulfur. In the copper alloying case, the temperature of the maximum moves from 480 to 645 K when the copper content is increased from 0 to 25 at.%. The apparent activation energies for r_1 and r_2 at low temperatures are in the range 200–210 and 243–285 kJ/mol, respectively, independent of the bulk copper content, x. The x dependence of r_1 and r_2 deviates significantly from a $(1-x)^n$ dependence, in contrast to the results of Dalmon and Martin (11). In the present case the influence of copper is much better described by a factor θ_H^n, where θ_H is the hydrogen capacity of the reduced $NiCu/SiO_2$ catalysts measured by Bernardo *et al.* (15) and shown in Table 1. The n values obtained for the temperatures 553, 573, and 593 K are in the range 1–3 and 2–3 for r_1 and r_2, respectively. Assuming that θ_H is proportional to the concentration of surface nickel atoms also during reaction, we may conclude from the point of view of an ensemble interpretation that the present sulfur chemisorption and the copper alloying experiments indicate a similar small ensemble requirement for a small ensemble for the hydrogenolysis of propane on the $Ni/MgAl_2O_4$ and on the $NiCu/SiO_2$ catalysts.

The silica-supported nickel–copper catalysts used by Dalmon and Martin (11) differ from our nickel–copper catalysts in the sense that Dalmon (19) concluded from magnetic and hydrogen chemisorption measurements that the surface of the reduced nickel–copper particles was not enriched in copper; i.e. the surface and bulk compositions were the same. This result is in contrast to most other published studies of supported and unsupported nickel–copper alloys. It is generally observed that surfaces of nickel–copper alloys are enriched in copper (at least in vacuum or in hydrogen). For comparison, the normalized hydrogen chemisorption results obtained on our $NiCu/SiO_2$ catalysts and the ones of Dalmon (19), used in Ref. (11), are plotted versus the bulk copper concentration x in Fig. 6 together with similar results reported by Sinfelt *et al.* (3) for unsupported NiCu particles. It is seen that our results for strongly adsorbed hydrogen show almost the same behavior as the

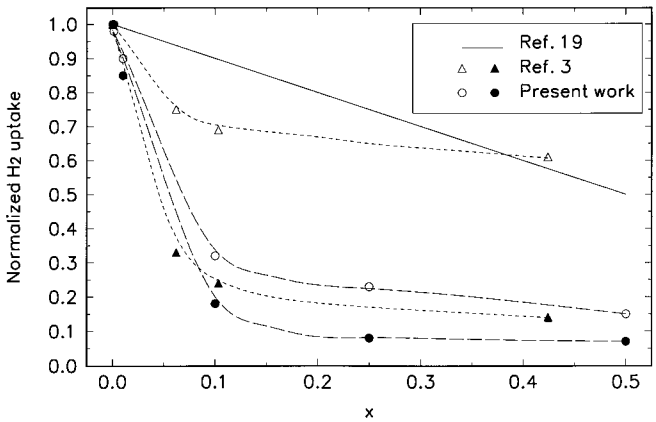

FIG. 6. Normalized hydrogen uptake on NiCu catalysts. (—) Total H_2 adsorption on $NiCu/SiO_2$ catalysts, Ref. (19). (△) Total adsorbed H_2 on unsupported NiCu, Ref. (3). (▲) Strongly adsorbed H_2 on unsupported NiCu, Ref. (3). (○) Total adsorbed H_2 on $NiCu/SiO_2$ catalysts, present work. (●) Strongly adsorbed H_2 on $NiCu/SiO_2$ catalysts, present work.

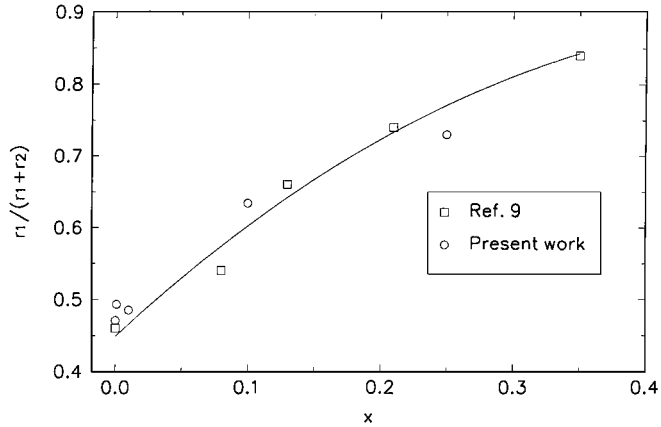

FIG. 8. Propane hydrogenolysis selectivity on $NiCu/SiO_2$ catalysts from Ref. (11), (□, 504 K) and present work (○, 553 K).

ones of Sinfelt *et al.* (3), i.e. reflecting a strong copper enrichment in the surface, while the results from Ref. (19) indicate that the surface and bulk have the same copper concentration.

It is tempting to believe that a comparison of the present propane hydrogenolysis results and the ones of Dalmon and Martin (11) would reveal a similar strong difference between the copper dependencies. Such a difference might be explained by a difference in surface segregation. However, the plots in Fig. 7 of the normalized rates of propane hydrogenolysis from the present study versus the bulk copper content together with the results of ethane and propane hydrogenolysis obtained by Dalmon and Martin (11) show a surprisingly good agreement. Only at about $x = 0.1$ are

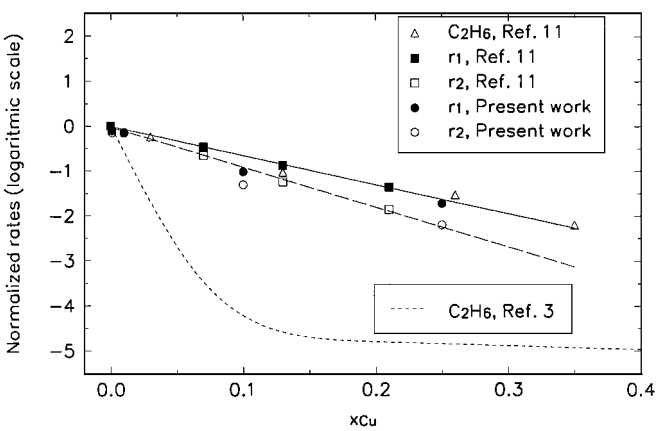

FIG. 7. Propane and ethane hydrogenolysis rates on $NiCu/SiO_2$ catalysts as functions of the Cu/(Ni + Cu) bulk ratio x. Ethane turnover numbers (503 K) from Ref. (11) (△), propane turnover numbers (540 K) r_1 (■) and r_2 (□) from Ref. (11). (△) Propane turnover numbers (553 K) r_1 (●) and r_2 (○) from the present work.

significant deviations seen. Also, the normalized rates of ethane hydrogenolysis from Ref. (3) are shown. Figure 7 shows that the rates of ethane and propane hydrogenolysis from Ref. (11) have the same x dependence, while the rate of ethane hydrogenolysis from Ref. (3) drops faster for small x values. On the basis of the similarity between our hydrogen chemisorption results and the ones in Ref. (3) we expect that our hydrogenolysis rates would also drop fast with x, contrary to the behavior seen in Fig. 7. Figure 8 shows that the selectivities obtained by Dalmon and Martin (11) and the ones obtained in the present work are also in very good agreement.

This agreement indicates that the differences in surface compositions as seen in the prereaction characterizations of the silica-supported nickel–copper catalysts may be partly leveled out during the hydrogenolysis reaction. However, the suggestion that the prereaction differences in surface compositions between differently prepared silica-supported nickel–copper catalysts disappear during reaction makes it difficult to explain the strong differences between the normalized ethane hydrogenolysis results of Sinfelt *et al.* (3) and those of Dalmon and Martin (11).

There are two major differences between the alloy catalysts used by Sinfelt *et al.* (3) and those used by Dalmon and Martin (11). The former catalysts were unsupported and the particle sizes were about 100 times larger than those of the latter catalysts. The most obvious explanation is therefore that the supply of copper atoms from the bulk to the surface is limited at the lower bulk copper concentrations for the supported catalysts, but not for the unsupported catalysts. The ratio of surface to bulk atoms is in the range 10–20% for the particles of the silica-supported catalysts, but of the order of 0.1% for the particles of the unsupported catalysts.

A contributing factor could also be different relative areas of (111), (100), and (110) orientations for the different types of catalysts. A larger part of the surfaces of the big

unsupported particles is expected to have (111) orientation compared with the surfaces of the small particles of the supported catalysts. Investigations of copper deposited on Ni(110), Ni(111), and Ni(100) indicate a very different behavior. On Ni(110), a three-layer deep alloying takes place (20), on Ni(111) surface alloying may not be possible (21), and on Ni(100) small stripes of embedded copper wedges are formed (22). The structure and composition of the surface formed by deposition of copper on the Ni(110) surface were the same as those of the surface formed by copper segregation to the (110) surface of a nickel–copper alloy (20). A possible explanation for the difference between the data of Dalmon and Sinfelt could be that a larger part of the surface of big nickel particles consists of (111) planes than of the surface of small particles. Because surface alloying does not take place on these planes, the surface energy may be lowered by the planes being covered by copper.

4.5. Ensembles or Special Sites?

Although it may be possible to understand the differences between the present and previous alloy results in the framework of an advanced ensemble model, as indicated above, there are other results which are more difficult to explain by means of an ensemble model. A clear understanding of the observed influences of support, particle size, adatom coverage, and alloying on hydrogenolysis activity may not be possible before a detailed description of the active surface during reaction is available, e.g., through *in situ* microscopy.

Ensemble models have often been used to explain structure-sensitive reactions as indicated above. In many cases surprisingly large ensemble sizes result from such analysis. It is not possible to reconcile the sulfur coverage and the alloying results above using a simple ensemble model based on the assumption of random distribution of the blocking agents. The extra assumptions needed are not easily quantified and justified.

As mentioned above, Burke and Ko (16) showed that it is possible to prepare nickel catalysts which have the same mean particle size, but different metal surface structures. The one with a large proportion of smooth (111) planes had a much lower activity than the one with many surface defects. This result shows that one cannot predict the specific hydrogenolysis activity from a knowledge of the mean particle size. More structural information is needed. However, experiments indicate that if the particle size is the only parameter to be changed, then the smaller particles result in higher specific hydrogenolysis activities. These observations are both in disagreement with ensemble model predictions.

In this connection, it is interesting that recently Dahl *et al.* (23) showed that the dissociation of N_2 on the close-packed Ru(0001) single-crystal surface is completely dominated by reaction on steps. Further work (24) indicates that sites similar to the step sites are present also on the nanoparticles of supported Ru catalysts.

In hydrogenolysis it is generally assumed that the rate-determining step consists of breaking a strong bond, viz., a C–C bond, similar to the N–N bond. It is therefore likely that defect sites dominate the catalytic activity also in the case of hydrogenolysis. This hypothesis provides a simple explanation for some of the observations mentioned above. It makes it easy to understand why particles with a high concentration of defects have a higher reactivity than particles with a high proportion of smooth surface planes, and that the hydrogen capacity of NiCu alloys does not correlate with hydrogenolysis activity. Also the support effects can readily be understood as caused by poisoning of the active sites.

5. CONCLUSIONS

The activity and selectivity of propane hydrogenolysis have been studied on nickel catalysts modified by sulfur chemisorption and copper alloying. In general, it is found that the ethane production rate goes through a maximum with increasing temperature. The selectivity increases as a function of sulfur coverage at low coverages and decreases again at high ones. The selectivity increases with increasing copper content in the copper range considered (0–25 at.%). The turnover numbers are significantly higher on the silica-supported than on the magnesium–aluminum–spinel-supported nickel catalysts. The results for the sulfur-modified catalysts indicate small ensemble requirements for propane hydrogenolysis. The results for the nickel–copper catalysts correspond to similar small ensembles if surface enrichment in copper is assumed. The ratios of ensemble sizes derived for reactions [1] and [2] are in disagreement with the observed sulfur and copper dependencies of selectivity, indicating that it is hardly influenced by ensemble effects. Comparisons with the results of a previous study of propane hydrogenolysis on silica-supported nickel–copper alloy catalysts, Ref. (11), reveal that the strong difference in copper dependence of the hydrogen capacity of the freshly reduced catalysts of Ref. (11) and those of the present work does not result in significant differences in the copper dependence of the hydrogenolysis rates or selectivity. This is unexpected because it was reported in Ref. (3) that the hydrogen uptake as well as the ethane hydrogenolysis rates of the unsupported NiCu depend strongly on the copper content. These results as well as other hydrogenolysis results question the use of ensemble models for the interpretation of hydrogenolysis results. The breaking of the strong C–C bonds may require special sites in analogy with the recent discovery that the dissociation of N_2 on ruthenium requires special sites.

REFERENCES

1. Carter, J. L., Cusumano, J. A., and Sinfelt, J. H., *J. Phys. Chem.* **70**, 2257 (1966).
2. Sinfelt, J. H., *Catal. Rev.* **3**, 175 (1969).
3. Sinfelt, J. H., Carter, J. L., and Yates, D. J. C., *J. Catal.* **24**, 283 (1972).
4. Boudart, M., *Adv. Catal.* **20**, 153 (1969).
5. Ponec, V., *Adv. Catal.* **32**, 149 (1983).
6. Andersen, N. T., Topsøe, F., Alstrup, I., and Rostrup-Nielsen, J. R., *J. Catal.* **104**, 454 (1987).
7. Alstrup, I., and Andersen, N. T., *J. Catal.* **104**, 466 (1987).
8. Martin, G. A., *J. Catal.* **60**, 345 (1979).
9. Guilleux, M. F., Dalmon, J. A., and Martin, G. A., *J. Catal.* **62**, 235 (1980).
10. Rostrup-Nielsen, J. R., *J. Catal.* **85**, 31 (1984).
11. Dalmon, J. A., and Martin, G. A., *J. Catal.* **66**, 214 (1980).
12. Rostrup-Nielsen, J. R., Catalytic Steam Reforming, *in* "Catalysis, Science and Technology" (J. R. Anderson and M. Boudart, Eds.), Vol. 5, p. 44. Springer, Berlin, 1983.
13. Alstrup, I., Rostrup-Nielsen, J. R., and Røen, S., *Appl. Catal.* **1**, 303 (1981).
14. Gorring, R. L., and De Rosset, A. J., *J. Catal.* **3**, 341 (1964).
15. Bernardo, C. A., Alstrup, I., and Rostrup-Nielsen, J. R., *J. Catal.* **96**, 517 (1985).
16. Burke, P. A., and Ko, E. I., *J. Catal.* **116**, 230 (1989).
17. Jackson, S. D., Gordon, J. K., and Webb, G., *Phys. Chem. Chem. Phys.* **1**, 2581 (1999).
18. Blackmond, D. G., and Ko, E. I., *J. Catal.* **96**, 210 (1985).
19. Dalmon, J. A., *J. Catal.* **60**, 325 (1979).
20. Rogge, V., and Neddermeyer, H., *Phys. Rev. B* **40**, 7559 (1989).
21. Voigt, J., Ding, X. L., Fink, R., Krausch, G., Luckscheiter, B., Platzer, R., Wöhrmann, U., and Schatz, G., *Phys. Rev. Lett.* **66**, 3199 (1991).
22. Rasmussen, F. B., Baker, J., Nielsen, M., Feidenhans'l, R., and Johnson, R. L., *Phys. Rev. Lett.* **79**, 4413 (1997).
23. Dahl, S., Logadottir, A., Egeberg, R. C., Larsen, J. H., Chorkendorff, I., Törnqvist, E., and Nørskov, J. K., *Phys. Rev. Lett.* **83**, 1814 (1999).
24. Dahl, S., Sehested, J., Jacobsen, C. J. H., Törnqvist, E., and Chorkendorff, I., *J. Catal.*, in press.